

Traveling Wave Model Based Simulation of Tunable Multi-Wavelength Diode Laser Systems

J.-P. Koester^{*†}, M. Radziunas[†], A. Zeghuzi^{*}, H. Wenzel^{*} and A. Knigge^{*}

^{*}Ferdinand-Braun-Institut, Leibniz-Institut für Höchstfrequenztechnik, Gustav-Kirchhoff-Str. 4, 12489 Berlin, Germany.

[†]Weierstrass Institute for Applied Analysis and Stochastics, Mohrenstr. 39, 10117 Berlin, Germany.

[‡]Email: jan-philipp.koester@fbh-berlin.de

Abstract—We show simulation results of a compact, integrated and tunable multi-wavelength diode laser emitting around 785 nm. The presented design was optimized using passive waveguide simulations and then further analyzed by performing active laser simulations. The latter enables deducing critical design parameters not accessible via an all-passive simulation.

I. INTRODUCTION

Tunable multi-wavelength GaAs-based diode lasers emitting in the wavelength range between 630 nm and 1.1 μm are of interest for several applications, for example Raman spectroscopy (785 nm), water vapor sensing (9xx nm), generation of THz radiation (830 nm) and optical coherence tomography (1064 nm). One possibility to realize such devices is to integrate two or more distributed feedback (DFB) or distributed Bragg reflector (DBR) lasers with different emission wavelengths next to each other on a chip and to couple the emission of each laser into one common output waveguide. This approach which is very common in the InP world (1.55 μm) can not easily be transferred to GaAs based devices because the needed multi-step epitaxy or heterogeneous integration is technologically much more challenging.

Our approach to fabricate tunable multi-wavelength lasers emitting at 785 nm avoids any multi-step epitaxy. The active region extends over the whole chip. The functionality of the different parts such as laser, amplifiers, waveguides and couplers are defined by etching parts of the surface of the chip and choosing appropriate contact layouts. Tuning is achieved by micro-heaters placed next to the lasers.

In our current designs the etch depth to form ridge waveguides for lateral optical confinement is the same over the whole chip [1] resulting in a long coupler section. To make the coupler section more compact we propose a new design based on realizing two etch depths. The regions where optical gain is supplied (lasers and amplifiers) are shallowly etched to ensure fundamental lateral mode operation. In contrast, the coupler section is deeply etched to provide a strong confinement.

II. DESIGN APPROACH

Our lateral-longitudinal design schematically shown in Fig. 1 can be divided into three sections. Starting from the left, a multi-channel section (MCS) consisting of DBR and active sections, the coupler section (CS) which connects all channels to one common output waveguide and, finally, the front section (FS). The regions depicted in bright gray are shallowly

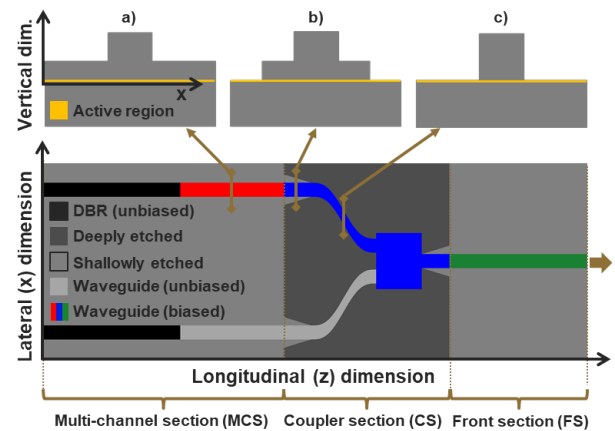


Fig. 1. Bottom: Lateral-longitudinal (x - z) plane of the device under study indicating the three different sections. Top: Vertical-lateral cross sections at different longitudinal positions. (a) Low confinement waveguide; (b) Waveguide taper; (c) High confinement waveguide

etched areas with an index contrast of $\Delta n_{\text{eff},s} = 3 \cdot 10^{-3}$, whereas the deeply etched regions with an index contrast of $\Delta n_{\text{eff},d} = 3 \cdot 10^{-2}$ are indicated by dark gray.

The CS consists of three different building blocks: First, mode converters formed by adiabatic linear tapers between the shallowly and deeply etched regions keeping the ridge width constant. Second, a multi-mode interference (MMI) coupler (in contrast to a Y-coupler used in e.g. [1]) to combine all laser channels to one common output waveguide. Third, sine-like S-bends to join the lasers and the coupler.

III. SIMULATION TOOLS

For the passive waveguide simulations we use the commercially available simulation tool FIMMWAVE [2] to optimize the building blocks introduced in Section II. It provides a rigorous and fully vectorial solution of Maxwell's equations in frequency domain based on an eigenmode expansion and a scattering matrix method.

Active laser simulations are performed using WIAS BA-Laser [3]. Its optical model provides an approximate solution of Maxwell's equations in the time domain. The forward and backward traveling slowly varying fields $u^{\pm}(x, z, t)$ within the lateral-longitudinal (x, z) plane are described by paraxial traveling wave equations coupled to equations governing the transport of the charged carriers [4]. The carrier transport

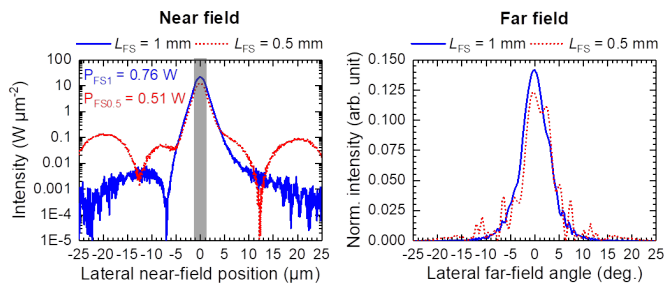


Fig. 2. Near- (left, logarithmic y-axis) and far-field (right) intensity profiles. Laser with long/short front section are shown as blue-solid/red-dotted lines.

model includes the lateral drift-diffusion of excess carriers within the active region modeled by an effective diffusion factor and current spreading inside the p-doped region modeled via the Laplace equation [5].

IV. RESULTS

First FIMMWAVE has been used to optimize the dimensions of the building blocks within the CS regarding low losses of the fundamental mode and negligible excitation of higher order modes. All following design parameters were obtained for a ridge waveguide width of 2.2 μm. The mode converter has a length of 100 μm where the width of the shallowly etched region changes linearly from 0 to 8 μm. To achieve a lateral offset of 40 μm the sine-like S-bend must have a length of 470 μm. Having a width of 12 μm the MMI coupler is calculated to be 330 μm long.

For the laser simulations the length and the coupling coefficient of the DBR were set to 1000 μm and $\kappa = 20 \text{ cm}^{-1}$, respectively. The electrically driven part of the MCS was 750 μm long. Two different lengths of the FS (500 μm and 1000 μm) were investigated. The front facet reflectivity was set to be 3 %.

In what follows we consider the case where only the upper of the two laser channels is electrically driven, applying voltages of 2.5 V, 1.7 V and 3.5 V to the gain section of the MCS, the CS and the FS, respectively. The corresponding areas are color-coded within Fig. 1. The CS voltage of 1.7 V is estimated to result in a carrier density slightly above transparency ($N_{tr} = 1.4 \cdot 10^{24} \text{ m}^{-3}$). All results shown below are based on time averaged values obtained between 2 ns and 3 ns after switching on all voltages.

Fig. 2 shows the near- and far-field intensity profiles emitted at the differently long FSs indicated by the right arrow in Fig. 1. Within and close to the waveguide (gray bar) both lengths of the FS lead to similar near-field profiles. Further away from the waveguide the laser with the shorter FS shows distinct side peaks. This, in turn, results in a modulated far-field profile.

The origin of this effect is visible from the intensity distributions shown in Fig. 3. A fraction of the guided light which propagates from the upper laser channel into the MMI is not coupled into the common output waveguide but radiated. This radiated light propagates forward and eventually reaches the front facet leading to the modulated far field profile. Since the

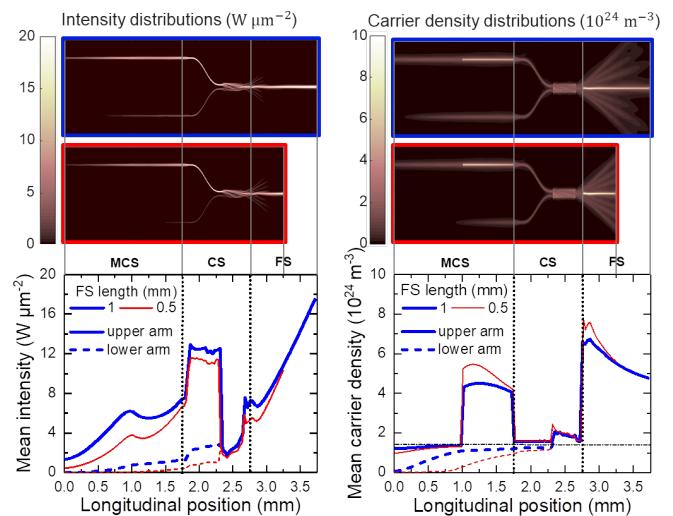


Fig. 3. Top: Intensity (left) and carrier density (right) distributions. Bottom: Longitudinal profiles in the upper (solid) and lower (dashed) channels.

areas next to the waveguide are unbiased, the radiated light gets absorbed within the active region creating electron-hole pairs, until transparency is reached. This effect leads to a fan-like carrier density distribution within the FS. In case of an FS length of 1000 μm most of the radiated light gets absorbed before reaching the front facet.

In addition to the shown (x,z)-distributions the effects caused by the guided light can be further characterized by longitudinal mean intensity and carrier density profiles obtained by laterally averaging over the e^{-2} -width of the fundamental guided mode. Both distributions indicate that a part of the backward traveling light is coupled into the unbiased lower channel where it gets absorbed. This happens within smaller distances for the laser with shorter FS. Nevertheless, both lasers provide negligible feedback from the lower unbiased laser channel back to the FS. As intended, the mean carrier density of the CS reaches values slightly higher than N_{tr} . The other sections, namely MCS and FS, show longitudinal spatial hole burning effects which are more pronounced for the laser with short FS.

V. CONCLUSION

Active laser simulations proved to be vital to understand the insides of multi-wavelength tunable laser. In addition, the promising results confirm our two etch step design approach, resulting in a more compact coupler section. Furthermore, we showed that a properly designed front section length can be used to avoid the appearance of far-field modulations by preventing that radiated light reaches the front facet.

REFERENCES

- [1] B. Sumpf et al. In *Novel In-Plane Semiconductor Lasers XVI*, volume 10123, page 101230T. Proc. of SPIE, 2017.
- [2] Photon Design®. FIMMWAVE. <https://www.photond.com/products/fimmwprop.htm>.
- [3] Weierstrass Institute Berlin. WIAS BALaser. <https://www.wias-berlin.de/software/balaser>.
- [4] M. Radziunas and R. Čiegis. *Math. Model. Anal.*, 19(5):627–646, 2014.
- [5] A. Zeghuzi et al. *IEEE J. Quantum Electron.*, 55(2):1–7, 2019.